Progress in Wide Area Methane Mapping for Application in the Energy Sector

William D. Tandy Jr., Jarett L. Bartholomew, Lyle Ruppert, Jeremy Craner, Steve Karcher, Carl S. Weimer, Philip C. Lyman, and P.R. Wamsley
Ball Aerospace, 1600 Commerce Street, Boulder, CO 80301
jbartholo@ball.com

Abstract: We report on advances in airborne differential absorption LIDAR that enable remote sensing of methane at spatial scales relevant to the energy sector. These observations bridge the gap between *in situ* and satellite observations.
OCIS codes: Remote Sensing and Sensors (280.0280); Air Pollution Monitoring (280.1120); Differential Absorption LIDAR (280.1910)

1. Introduction

Starting with a DOT/PHMSA award in 2013, Ball has been partnering with government and industry partners to develop a next-generation airborne sensor capable of taking 10,000 measurements per second on an airborne platform a kilometer above industry assets with a wide-area swath width of 300 meters [1,2]. The team continues to improve from this foundation. This paper presents some of the most recent efforts and observations.

2.0 Hardware Improvements

Recent field and laboratory work showed that laser pulses that vary in length can drive non-linear responses in the detector chain. Nominally, pulses are on the order of 30 ns. However, terrain, structures, vegetation, and pointing angle can skew the pulse returns to be up to 100% longer. A detector with mismatched bandwidth will stretch the shorter pulses differently than it stretches longer pulses. An amplifier and/or filter in the detector chain can exacerbate the issue with additional non-linear bandwidth response. Unfortunately, using a higher bandwidth (faster) detector and amplifier typically introduces additional noise. Another common approach is to bias the detector with a voltage to reduce the substrate capacitance, but this introduces dark current noise.

In the last few months, Ball Aerospace has simulated optimal responses and tested a wide variety of bandwidth combinations. The hardware side of the trade study included both extremes of bandwidth with both faster (35 MHz) and slower detectors (10 MHz) than what simulation predicted would be best. Electronic filters tested after the detectors ranged from 14 MHz to 30 MHz. Finally, amplifiers after the receiver detector ranged from 10 to 100 MHz. The matrix of tests combined every set of parameters including the in-between cases, such as pairing a fast detector with a slow filter, or putting a slow detector on the gas cell measurement and fast detector on the receive side. Testing took place both in the laboratory and in field work at the NOAA Table Mountain facility just north of Boulder, Colorado.

The conclusion was the fastest detectors performed the best, even though common guidelines and simulation showed that the higher bandwidth was not required. There was interest in testing even faster detectors, but detector size requirements on the receiver limited this effort. Further, it was found that the introduced noise from biasing and the detector's higher bandwidth introduced negligible noise if a middle of the road bandwidth was used on the passive filter. A value of 21 MHz was used. The amplifier chosen runs at 100 MHz. Interestingly, this has half the gain of the previous version, which ran at 10 MHz. The concern was that lower gain could mean lower flight altitude and thus reduced swath width. However, testing showed that the improved following of the signal's peak with the faster amplifier recovered sufficient signal to overcome the gain loss. Additionally, for the system as a whole, we traded bandwidth noise for amplifier noise which is "whiter" and averages better.

3.0 Instrument Software Improvements

The software used to process data is covered in Steve Karcher's recent National Instruments' paper and in the recently published hardware paper [1,2]. Since publishing, improvements have been made to optimize the software chain for commercial operations.

The user interface's "Viewer" software has recent updates that reduce the work load on the operator. For instance, the instrument has been designed to point the laser to follow pipelines defined by Google's Keyhole Markup Language (KML) files. The software now tracks in real-time which targets have been covered using the real-time georectification algorithms. It does this by breaking a survey line up into 1-meter segments and checking which have been covered with at least 4-meters of data on either side of the pipeline. This is displayed graphically and in tabular form, making it much easier for the operator to work with the pilot to achieve mission goals.

Another helpful improvement to the software is the inclusion of laser pulse energy histograms in the main interface. A previous iteration of the software chain required the operator to flip between programs to view this information. Bringing in real-time counts of laser pulse energy to the same screen as the other data may seem small, but it greatly simplifies understanding the health of the system. It also facilitates onboard optimization of instrument settings. Similarly, new plots of intermediary data, such as gas cell readings, allows for finer understanding of how the system is performing from the single screen.

Improvements to automatically cleaning out "bad" data are ongoing. Rudimentary approaches have been in place since the beginning of commercial operations. For instance, if a pulse comes back without a well-defined shape due to, perhaps, interaction with trees or water, the data are flagged as bad and not shown to the operator. (Note that these data are still saved for possible post-processing on the ground.) The latest round of changes now brings more control over the range of pulse shapes filtered to the user interface. The ability to fine-tune in the air and receive real-time feedback accommodates diverse types of terrains and target topologies.

4.0 Post-Processing Improvements and Examples

Post-processing takes place in two locations: as part of the capabilities of the Viewer software and on Ball's High-Performance Cluster (HPC) with 320 CPU cores and highly parallelized code. Typically, development algorithms are tested on the HPC and then ported to Viewer when proven reliable. One example is the real-time data smoothing process. It uses the range adjusted methane values in a Gaussian weighted algorithm that scales the weights with distance from a point. Recent trade studies show that the optimal radius for the Gaussian equation is between 5 and 10 meters. Another addition is the ability to use custom ranges in Viewer to isolate potential plumes to just the levels of concern. For instance, if a customer is only interested in the largest plumes then those can be specifically searched for in the hundreds of GB of data.

One ongoing effort on the HPC side is plume analysis. Figure 1 below shows a plume found in northeast Colorado. Although clearly a plume, the lumpiness could seem to make leak rate determination difficult. Analysis of the underlying data, though, shows that in the cross-axis direction the plume's width closely follows Gaussian plume simulations [3,4]. The middle and right-side plots in Figure 1 show the raw data within 5-meter bins near the plume source fit to a Gaussian curve. The R^2 values for these fits are better than 90% demonstrating the utility of the Gaussian plume when there is sufficient spatial sampling of the plume.

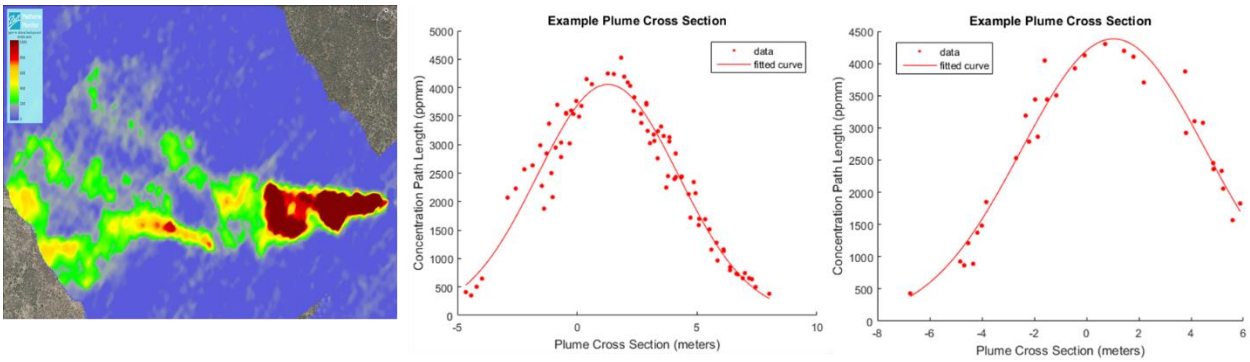

Figure 1: Example real-world plume and its cross-sections measured with Ball's methane detecting instrument. The cross-sections are Gaussian fits as described in a Gaussian plume model.

These improvements were tested in the field and applied to commercial operations in September 2017. Figure 2 shows a plume release of 800 SCFH with a 300-meter instrument swath width. The house on the left-hand side demonstrates the scale of both the swath width and the plume. Capturing the entire plume in this way provides a much-improved ability to confirm the plume signal, quantify the leak rate, and determine wind direction.

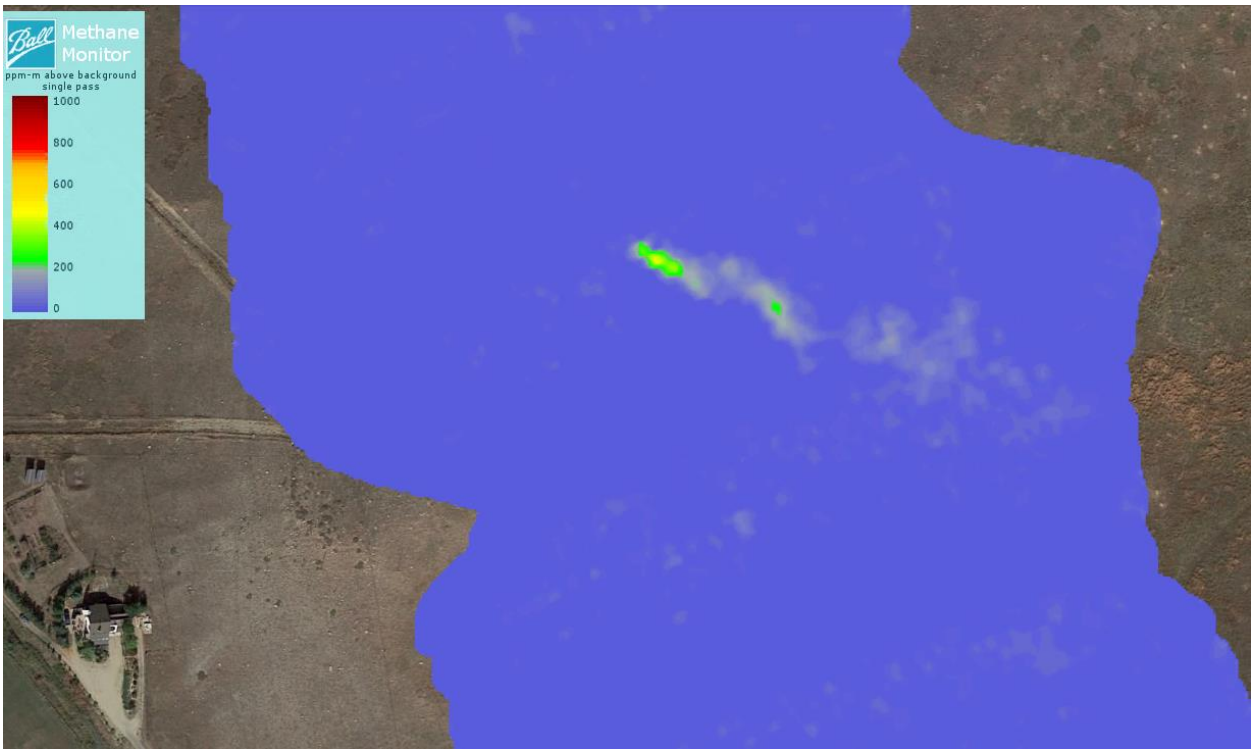

Figure 2: Example post-processed display of an 800 SCFH plume taken during Ball trials in September 2017. The house on the left side demonstrates the scale of the instrument's swath width.

5.0 Conclusions and Future Work

Ball Aerospace continues to fine-tune the hardware and software used to search for methane emissions. Upcoming hardware work includes modifications to the instrument to fit in a variety of aircraft, testing a change to the laser pick-off system used signal normalization, and optimizing the diffuser system on the transmit side. The largest software work will focus on tightening feedback to the pilot to allow for more flexible field operations. For instance, providing the optimal flight route to cover pipeline and survey targets while minimizing wasteful aircraft turns. Integrating ADS-B, the next generation of aircraft tracking hardware, into the pilot's screen is also in-work to increase safety and situational awareness for the team.

6.0 Acknowledgements

The accomplishments reported here were made possible through funding from the DOT/PHMSA R&D Program awards DTPH5613T000004 and DTPH5615T00016. Additional support comes from Ball Aerospace, energy industry partners, and a Technical Advisory Committee comprised of stakeholders.

7.0 References

[1] Jarett Bartholomew, Philip Lyman, Carl Weimer, William Tandy, "Wide area methane emissions mapping with airborne IPDA lidar", Proc. SPIE 10406, Lidar Remote Sensing for Environmental Monitoring 2017, 1040607 (2017/08/30); doi: 10.1117/12.2276713

[2] S. Karcher, "Embedded DIAL System for Measuring Fugitive Natural Gas Emissions" NIWeek, http://sine.ni.com/cs/app/doc/p/id/cs-17379#, (2017).

[3] Roberts, O. F. T. "The theoretical scattering of smoke in a turbulent atmosphere." *Proceedings of the Royal Society of London. Series A, Containing Papers of a Mathematical and Physical Character* 104.728 (1923): 640-654.

[4] Sutton, O. G. "The theoretical distribution of airborne pollution from factory chimneys." *Quarterly Journal of the Royal Meteorological Society* 73.317- 318 (1947): 426-436.